Nonlinear Full-Model-Based Controller for Unactuated Joints in Vertical Plane

Nonlinear Full-Model-Based Controller for Unactuated Joints in Vertical Plane

Pauli Mustalahti
Laboratory of Automation and Hydraulic Engineering
Tampere University of Technology
Tampere, Finland FI-33101
firstname.lastname@tut.fi

Jouni Mattila
Laboratory of Automation and Hydraulic Engineering
Tampere University of Technology
Tampere, Finland FI-33101
firstname.lastname@tut.fi

***Abstract*—Articulated multiple degrees-of-freedom (DOF) hydraulic manipulators are used in many industry tasks. These hydraulic manipulators can be used to move heavy loads, such as logs and containers. The grasping tool of these manipulators is often connected at the tip of the manipulator by using unactuated revolute joints, which are not directly controllable. Currently, work performed efficiently by commercial hydraulic manipulators depends on the driver, and the automation level of these manipulators is relatively low. The Virtual Decomposition Control (VDC) is the nonlinear model-based control theory, which performs subsystem-based control design and stability analysis for complex multiple DOF redundant hydraulics manipulators. In this paper, we present a VDC approach-based nonlinear full-model-based anti-sway controller for a redundant manipulator in vertical plane. The experimental results, with a full-size redundant hydraulic manipulator, verify that the proposed anti-sway control efficiently damps load swaying in the vertical plane motions.**

I. Introduction

In industry, commercial hydraulic manipulators are used in different tasks to move heavy loads, such as logs, biomass and containers. Often, the grasping tool of the manipulator is connected at the tip of the manipulator via a pair of unactuated revolute joints to enable effective grasping. In free-space, these unactuated joints sway due to the tip accelerations. Because passive joints are not directly controllable, only the operator can ensure the safe motions.

The operator workloads can be decreased and safety can be increased by designing robotic controllers for the manipulators. As discussed in a survey of control hydraulic robotic manipulators [1], robotics control for the heavy-duty manipulators is expected to revolutionize control of these machines. The first commercial boom tip control solutions for heavy-duty hydraulic manipulators are available (see [2], [3]). However, commercial solutions for hydraulic manipulators to control a freely swaying load are not yet available.

The highly nonlinear dynamics behavior of hydraulic manipulators makes their high-performance control design task substantial [1]. In the literature, most of the proposed anti-sway control methods, e.g. [4]–[8], are still based on linear/linearized control methods, which leads to approximations in the controller and limited control performance. In addition, only a few proposed control methods have been verify with full-scale manipulators [8]–[10]. As the survey [1] presents, nonlinear model-based control methods produced high control performance. Only implemented nonlinear anti-sway control methods are presented in [9] and [10]. In [10] is proposed a nonlinear model predictive control for a 4-DOF hydraulic manipulator. However, some of the major nonlinearities in the system were neglected.

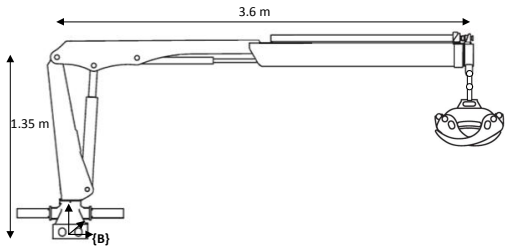

Fig. 1. Redundant hydraulic manipulator

Our previous study [9] proposed a theory for a nonlinear model-based anti-sway controller for underactuated redundant hydraulic manipulator by using Virtual Decomposition Control (VDC) approach. However, the control design still neglected the unactuated joint frictions and the torque constraints in unactuated joints. The present paper removes these assumptions and extends VDC to cover joint frictions and constraints in passive joints. Similar to [9], the tool (the gripper mass 90 kg + an additional load of 150 kg) is connected at the tip of the 4-DOF coordinate controlled redundant hydraulic manipulator as Fig. 1 presents. Experimental results demonstrate that the proposed controller yields a better control performance in relation to our previous study [9].

This paper is organized as follows. Section II introduces the basis of the VDC approach. Section III defines the kinematics and dynamics of the unactuated *open chain* and *object*, and Section IV presents corresponding control equations for these subsystems. Section IV defines releasing terms, which cover the force/torque constraints of the joints. The virtual stability of the unactuated *open chain* is presented in Section VI. Finally, experimental results are presented in Section VII, and conclusions are outlined in Section VIII.

II. Virtual Decomposition Control

The VDC approach (see [11], [12]) provides subsystem-based control design tools for robotic systems. Subsystem-based control design is suitable especially for complex robotic

systems with multiple DOF at the subsystem level. The subsystem-based control design can also be used to perform stability analysis of the system locally at the subsystem level. The VDC approach also enables the modular control design, because it is possible to add or replace one subsystem with another without changing the control equations of the other subsystems. Next, subsection II-A presents the basic mathematical notations of the VDC approach. Then, subsection II-B presents a virtual decomposition (a unique feature of VDC) of the system, a simple oriented graph (SOG) presentation, and a coordinate frame attachment in the studied subsystems.

A. Mathematical Notations

Consider a coordinate frame $\{\mathbf{A}\}$, which is fixed to the rigid body. According to [12], the linear/angular velocity vector in this frame can be defined by a combination of a linear velocity vector ${}^{\mathbf{A}}\mathbf{v} \in \mathbb{R}^3$ and an angular velocity vector ${}^{\mathbf{A}}\boldsymbol{\omega} \in \mathbb{R}^3$ as ${}^{\mathbf{A}}V = [{}^{\mathbf{A}}\mathbf{v} \quad {}^{\mathbf{A}}\boldsymbol{\omega}]^T$. Similarly, the force/torque vector, in coordinate frame $\{\mathbf{A}\}$, can be defined as a compilation of a force vector ${}^{\mathbf{A}}\mathbf{f} \in \mathbb{R}^3$ and a moment vector ${}^{\mathbf{A}}\mathbf{m} \in \mathbb{R}^3$ like ${}^{\mathbf{A}}F = [{}^{\mathbf{A}}\mathbf{f} \quad {}^{\mathbf{A}}\mathbf{m}]^T$. Now, the following transformations for the two fixed coordinate frames $\{\mathbf{A}\}$ and $\{\mathbf{B}\}$ holds:

$$ {}^{\mathbf{B}}V = {}^{\mathbf{A}}\mathbf{U}_{\mathbf{B}}^{T}\,{}^{\mathbf{A}}V \tag{1} $$

$$ {}^{\mathbf{A}}F = {}^{\mathbf{A}}\mathbf{U}_{\mathbf{B}}\,{}^{\mathbf{B}}F, \tag{2} $$

where ${}^{\mathbf{A}}\mathbf{U}_{\mathbf{B}} \in \mathbb{R}^{6\times 6}$ presents the force/moment transformation between the two fixed frames.

In view of [12], the dynamics equation in fixed coordinate frame $\{\mathbf{A}\}$ can be written as

$$ {}^{\mathbf{A}}F^{*} = \mathbf{M}_{\mathbf{A}}\frac{d}{dt}({}^{\mathbf{A}}V) + \mathbf{C}_{\mathbf{A}}({}^{\mathbf{A}}\boldsymbol{\omega})\,{}^{\mathbf{A}}V + \mathbf{G}_{\mathbf{A}}, \tag{3} $$

where $\mathbf{M}_A \in \mathbb{R}^{6\times 6}$ is the mass matrix, $\mathbf{C}_{\mathbf{A}}({}^{\mathbf{A}}\boldsymbol{\omega}) \in \mathbb{R}^{6\times 6}$ is the Coriolis and centrifugal terms, $\mathbf{G}_{\mathbf{A}} \in \mathbb{R}^6$ is the gravity vector, and ${}^{\mathbf{A}}F^{*} \in \mathbb{R}^6$ is the net force/moment vector. The required rigid body dynamics can be defined by using the linear parametrization expression as

$$ \mathbf{Y}_{\mathbf{A}}\boldsymbol{\theta}_{\mathbf{A}} \stackrel{\text{def}}{=} \mathbf{M}_{\mathbf{A}}\frac{d}{dt}({}^{\mathbf{A}}V_{\mathrm{r}}) + \mathbf{C}_{\mathbf{A}}({}^{\mathbf{A}}\boldsymbol{\omega})\,{}^{\mathbf{A}}V_{\mathrm{r}} + \mathbf{G}_{\mathbf{A}}, \tag{4} $$

where definitions for the regressor matrix $\mathbf{Y}_A \in \mathbb{R}^{6\times 13}$ and the parameter vector $\boldsymbol{\theta}_{\mathbf{A}} \in \mathbb{R}^{13}$ are presented in [12]. VDC control theory includes parameter adaption for parameters in $\boldsymbol{\theta}_{\mathbf{A}}$, but parameter adaption is not implemented in this paper.

B. Virtual Decomposition of the System

The first step of the VDC approach is a virtual decomposition of the system into subsystems (*objects* and *open chains*) by placing virtual cutting points (VCPs). A VCP is a directed separation interface that defines the direction for the force/moment relations with other subsystems and conceptually divides the rigid body. A VCP is simultaneously interpreted as a driven VCP by another subsystem and as a driving VCP by one subsystem. The driven VCP is a point to which the force/moment vector is exerted, and the driving VCP is a point from which the force/moment vector is exerted.

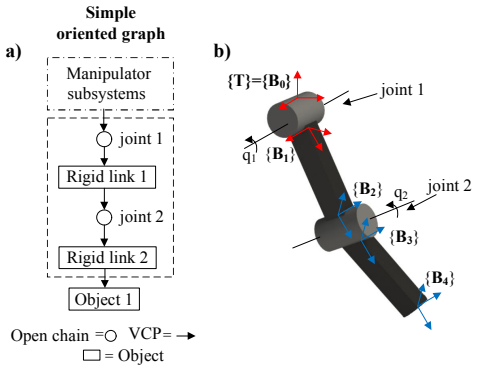

Fig. 2. Unactuated open chain

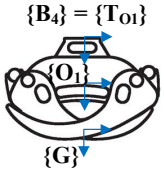

Fig. 3. Object

The dynamics relations between the subsystems can be presented by using a SOG (see Denition 2.14 in [12]). In a SOG, each VCP corresponds a directed edge, which defines the reference direction for the force/moment vector, and each subsystem is presented as a node. In a SOG, loops are not allowed [12]. The SOG for the studied unactuated *open chain* and *object* are presented in Fig. 2a. In this paper, the focus is to design control equations for the unactuated *open chain* inside the dashed line. The virtual decomposition for the 5-DOF hydraulic manipulator (the inside dash-dot line) is given in [9], and detailed control equations for a similar hydraulic crane are given in [13]. Because the connected load mass is subject to change, the load is modeled as a separate *object*. Thus, it is possible to change only the *object's* modeling parameters to correspond to the real system.

The kinematics and dynamics relations of the unactuated *open chain* and *object* are defined by using fixed coordinate frames in the rigid bodies. The attached frames for the studied subsystems are presented in Fig. 2b and Fig. 3. In frames $\{\mathbf{B}_0\}$ and $\{\mathbf{B}_1\}$, denoted with red, the z-axle points out from *joint* 1, and in frames $\{\mathbf{B}_2\}$, $\{\mathbf{B}_3\}$, and $\{\mathbf{B}_4\}$ the z-axis pointing out from *joint* 2.The coordinate frames for the *object* follow from the studied *open chain* frames; therefore, in Fig. 3 the z-axis pointing out from the paper. The other axes are defined according to the right-hand rule.

III. Kinematics and Dynamics of the Unactuated Open Chain and Object

This section defines the kinematics and dynamics equations for the unactuated *open chain* (see Fig. 2) and the *object* (see Fig. 3).

A. Kinematics Equations of the Unactuated Open Chain

In view of Fig. 2b and Eq. (1), the kinematics equations for the unactuated *open chain* can be written as

$$
\begin{aligned}
{}^{\mathbf{B}_1}V &= {}^{\mathbf{B}_0}\mathbf{U}_{\mathbf{B}_1}^T\,{}^{\mathbf{B}_0}V + \mathbf{z}\dot{q}_1 && (5)\\
{}^{\mathbf{B}_2}V &= {}^{\mathbf{B}_1}\mathbf{U}_{\mathbf{B}_2}^T\,{}^{\mathbf{B}_1}V && (6)\\
{}^{\mathbf{B}_3}V &= {}^{\mathbf{B}_2}\mathbf{U}_{\mathbf{B}_3}^T\,{}^{\mathbf{B}_2}V + \mathbf{z}\dot{q}_2 && (7)\\
{}^{\mathbf{B}_4}V &= {}^{\mathbf{B}_3}\mathbf{U}_{\mathbf{B}_4}^T\,{}^{\mathbf{B}_3}V, && (8)
\end{aligned}
$$

where $\mathbf{z} = [0\ 0\ 0\ 0\ 0\ 1]^T$ and $\dot{q}_i, \forall i \in \{1,2\}$ is the angular velocity of the ith joint.

B. Kinematics Equations of the Object

In view of Eq. (1) the linear/angular velocity vector of the *object* can be defined as

$$
{}^{\mathbf{O}_1}V = {}^{\mathbf{T}_{O1}}\mathbf{U}_{\mathbf{O}_1}^T\,{}^{\mathbf{T}_{O1}}V = {}^{\mathbf{G}}\mathbf{U}_{\mathbf{O}_1}^T\,{}^{\mathbf{G}}V. \tag{9}
$$

C. Dynamics Equations of the Object

The net force/moment vector for the *object* can be defined, in view of Eq. (3), as

$$
{}^{\mathbf{O}_1}F^* = \mathbf{M}_{\mathbf{O}_1}\frac{d}{dt}({}^{\mathbf{O}_1}V) + \mathbf{C}_{\mathbf{O}_1}({}^{\mathbf{O}_1}\omega)\,{}^{\mathbf{O}_1}V + \mathbf{G}_{\mathbf{O}_1}. \tag{10}
$$

Second, the force/moment resultant equation in the *object* can be written as

$$
{}^{\mathbf{O}_1}F^* = {}^{\mathbf{O}_1}\mathbf{U}_{\mathbf{T}_{O1}}\,{}^{\mathbf{T}_{O1}}F - {}^{\mathbf{O}_1}\mathbf{U}_{\mathbf{G}}\,{}^{\mathbf{G}}F, \tag{11}
$$

where the external force ${}^{\mathbf{G}}\boldsymbol{F}$ can be written as

$$
{}^{\mathbf{G}}\boldsymbol{F} = [0\ 0\ 0\ 0\ 0\ 0]^T \tag{12}
$$

in free-space motions.

D. Dynamics Equations of the Unactuated Open Chain

By reusing Eq. (3), the dynamics equations for both unactuated rigid bodies can be written as

$$
{}^{\mathbf{B}_j}F^* = \mathbf{M}_{\mathbf{B}_j}\frac{d}{dt}({}^{\mathbf{B}_j}V) + \mathbf{C}_{\mathbf{B}_j}({}^{\mathbf{B}_j}\omega)\,{}^{\mathbf{B}_j}V + \mathbf{G}_{\mathbf{B}_j}, \tag{13}
$$

where $j \in \{1,3\}$ is the order number of the link. Because the joint mass is low compared to the rigid links mass, the joint mass can be included in the links mass. In the studied coordinate frames, the total force/moment vectors can be written as

$$
\begin{aligned}
{}^{\mathbf{B}_3}F &= {}^{\mathbf{B}_3}F^* + {}^{\mathbf{B}_3}\mathbf{U}_{\mathbf{B}_4}\,{}^{\mathbf{B}_4}F + \mathbf{z}J_2\ddot{q}_2 && (14)\\
{}^{\mathbf{B}_2}F &= {}^{\mathbf{B}_2}\mathbf{U}_{\mathbf{B}_3}\,{}^{\mathbf{B}_3}F && (15)\\
{}^{\mathbf{B}_1}F &= {}^{\mathbf{B}_1}F^* + {}^{\mathbf{B}_1}\mathbf{U}_{\mathbf{B}_2}\,{}^{\mathbf{B}_2}F + \mathbf{z}J_1\ddot{q}_1 && (16)\\
{}^{\mathbf{B}_0}F &= {}^{\mathbf{B}_0}\mathbf{U}_{\mathbf{B}_1}\,{}^{\mathbf{B}_1}F, && (17)
\end{aligned}
$$

In Eqs. (14) and (16) the terms $J_1\ddot{q}_1$ and $J_2\ddot{q}_2$ are released to satisfy the torque constraints. These terms are defined more specifically in Section V.

The force constraints in the unactuated joints can be defined as

$$
\mathbf{z}^T\,{}^{\mathbf{B}_j}F + \tau_{f_i} = 0, \tag{18}
$$

where $j \in \{1,3\}$ is the order number of the frame, τ_{f_i} is the friction constraint for the relative joint, and $i \in \{1,2\}$ is the order number of the joint.

In this paper, the joint friction is modeled by using viscous and Coulomb friction coefficients. Therefore, the joint friction can be written as

$$
\tau_{f_i} = k_{vi}\dot{q}_i + k_{ci}\tanh(n\dot{q}_i), \tag{19}
$$

where k_{vi} is the viscous coefficient, k_{ci} is the Coulomb coefficient and $n > 0$ and constant.

IV. Control Equations of the System

This section presents the required linear/angular velocities for the *object* and the unactuated *open chain*. In addition, the required force/moment vectors for the studied subsystems are presented.

A. Required Kinematics Equations of the Unactuated Open Chain

By reusing Eq. (5)–(8), the required linear/angular velocity vectors can be written as

$$
\begin{aligned}
{}^{\mathbf{B}_1}V_r &= {}^{\mathbf{B}_0}\mathbf{U}_{\mathbf{B}_1}^T\,{}^{\mathbf{B}_0}V_r + \mathbf{z}\dot{q}_{1r} && (20)\\
{}^{\mathbf{B}_2}V_r &= {}^{\mathbf{B}_1}\mathbf{U}_{\mathbf{B}_2}^T\,{}^{\mathbf{B}_1}V_r && (21)\\
{}^{\mathbf{B}_3}V_r &= {}^{\mathbf{B}_2}\mathbf{U}_{\mathbf{B}_3}^T\,{}^{\mathbf{B}_2}V_r + \mathbf{z}\dot{q}_{2r} && (22)\\
{}^{\mathbf{B}_4}V_r &= {}^{\mathbf{B}_3}\mathbf{U}_{\mathbf{B}_4}^T\,{}^{\mathbf{B}_3}V_r, && (23)
\end{aligned}
$$

In view of [12], the required velocity consists of the desired velocity and terms that are related to control errors. Now, in Eq. (20) and (22), the required joint velocities for the unactuated joints can be defined as

$$
\dot{q}_{i\mathrm{r}} = \dot{q}_{i\mathrm{d}} + \lambda_{u_i}(q_{i\mathrm{d}} - q_i). \tag{24}
$$

In Eq. (24), λ_{u_i} is the position feedback gain for the relative joint. For unactuated joints, the desired joint velocity and position are usually designed according to the equilibrium point. When the *object* is symmetric, the desired joint velocity for both joints is 0 rad/s and the desired position is 0 rad.

B. Required Kinematics Equations for the Object

By reusing Eq. (9), the required kinematic equations for the *object* can be defined as

$$
{}^{\mathbf{O}_1}V_r = {}^{\mathbf{T}_{O1}}\mathbf{U}_{\mathbf{O}_1}^T\,{}^{\mathbf{T}_{O1}}V_r = {}^{\mathbf{G}}\mathbf{U}_{\mathbf{O}_1}^T\,{}^{\mathbf{G}}V_r. \tag{25}
$$

C. Required Dynamics Equations of the Object

By reusing Eq. (4), the *object's* required force/moment vector can be defined as

$$
{}^{\mathbf{O}_1}F_r^* = \mathbf{Y}_{\mathbf{O}_1}\theta_{\mathbf{O}_1} + K_{\mathbf{O}_1}({}^{\mathbf{O}_1}V_r - {}^{\mathbf{O}_1}V). \tag{26}
$$

In Eq. (26), $K_{\mathbf{O}_1}$ is the velocity feedback control gain matrix.

Furthermore, by reusing Eq. (11), the net force/moment vector in frame $\{\mathbf{T}_{\mathbf{O}_1}\}$ can be defined as

$$
{}^{\mathbf{T}_{O1}}F_r^* = {}^{\mathbf{T}_{O1}}\mathbf{U}_{\mathbf{O}_1}\,{}^{\mathbf{T}_{O1}}F_r - {}^{\mathbf{T}_{O1}}\mathbf{U}_{\mathbf{G}}\,{}^{\mathbf{G}}F_r, \tag{27}
$$

where the required external force vector

$$
{}^{\mathbf{G}}F_r = [0\ 0\ 0\ 0\ 0\ 0]^T \tag{28}
$$

is designed similarly to Eq. (12).

D. Required Dynamics Equations for the Unactuated Open Chain

The required dynamics equations for the unactuated *open chain* can be defined by using the required linear/angular velocity vectors in Eqs. (20)–(23) and by reusing Eq. (4) as

$$^{\mathbf{B}_j}F_r^* = \mathbf{Y}_{\mathbf{B}_j}\theta_{\mathbf{B}_j} + \mathbf{K}_{\mathbf{B}_j}(^{\mathbf{B}_j}V_r - ^{\mathbf{B}_j}V), \tag{29}$$

where $j \in \{1,3\}$ is the order number of the frame.

Thus, in view of Eqs. (14)–(17), the total required force/moment vectors are

$$^{\mathbf{B}_3}F_r = {}^{\mathbf{B}_3}F_r^* + {}^{\mathbf{B}_3}\mathbf{U}_{\mathbf{B}_4}{}^{\mathbf{B}_4}F_r + \mathbf{z}J_2\ddot{q}_{2r} \tag{30}$$

$$^{\mathbf{B}_2}F_r = {}^{\mathbf{B}_2}\mathbf{U}_{\mathbf{B}_3}{}^{\mathbf{B}_3}F_r \tag{31}$$

$$^{\mathbf{B}_1}F_r = {}^{\mathbf{B}_1}F^* + {}^{\mathbf{B}_1}\mathbf{U}_{\mathbf{B}_2}{}^{\mathbf{B}_2}F_r + \mathbf{z}J_1\ddot{q}_{1r} \tag{32}$$

$$^{\mathbf{B}_0}F_r = {}^{\mathbf{B}_0}\mathbf{U}_{\mathbf{B}_1}{}^{\mathbf{B}_1}F_r. \tag{33}$$

The required force constraints for unactuated joints can be defined, similar to Eq. (18), as

$$0 = \mathbf{z}^{T\,\mathbf{B}_j}F_r + \tau_{f_{ir}}, \tag{34}$$

where $j \in \{1,3\}$ is the order number of the frame, $\tau_{f_{ir}}$ is the required friction constraint for the relative joint, and $i \in \{1,2\}$ is the order number of the joint. The required friction constraint for the joints can be written by reusing Eq. (19) as

$$\tau_{f_{ir}} = k_{vi}\dot{q}_{ir} + k_{ci}\tanh(n\dot{q}_{ir}), \tag{35}$$

where $i \in \{1,2\}$ is the order number of the joint.

V. Definition of the Relasing Terms

In this section, the terms $J_i\ddot{q}_i$ and $J_i\ddot{q}_{ir}$ are defined, which are released to satisfy the force/moment constraints in Eqs. (18) and (34) in Eqs. (14), (16), (30), and (32), when $i \in \{1,2\}$ is the order number of the joint. As is discussed in [12], the number of the force/moment constraints is equal to the released variables. In this paper, the *open chain* consists of two unactuated joints; thus, the released variables to these joints are angular accelerations of the joints.

According to Eqs. (14), (16), and (18), the released terms for the joints can be written as

$$J_2\ddot{q}_2 = -\mathbf{z}^{T\,\mathbf{B}_3}F^* - \mathbf{z}^{T\,\mathbf{B}_3}\mathbf{U}_{\mathbf{B}_4}{}^{\mathbf{B}_4}F - \tau_{f_2} \tag{36}$$

$$J_1\ddot{q}_1 = -\mathbf{z}^{T\,\mathbf{B}_1}F^* - \mathbf{z}^{T\,\mathbf{B}_1}\mathbf{U}_{\mathbf{B}_2}{}^{\mathbf{B}_2}F - \tau_{f_1}. \tag{37}$$

Because in commercial manipulators joint angles are mechanically limited, the following assumption can be made:

Assumption 1. *An unactuated open chain cannot reach its unstable equilibrium point.*

According to Assumption 1, the joint angular acceleration is zero, when the joint is in an equilibrium point in a free-space motion. In the equilibrium point, the torque constraints (18) and (34) hold. When the angular acceleration is different from zero, the mapping coefficients J_2 and J_1 can be solved from Eqs. (36) and (37).

The required mapping coefficients according to Eqs. (30), (32), and (34) for the unactuated joints can be written as

$$J_{2r}\ddot{q}_{2r} = -\mathbf{z}^{T\,\mathbf{B}_3}F^* - \mathbf{z}^{T\,\mathbf{B}_3}\mathbf{U}_{\mathbf{B}_4}{}^{\mathbf{B}_4}F - \tau_{f_{2r}} \tag{38}$$

$$J_{1r}\ddot{q}_{1r} = -\mathbf{z}^{T\,\mathbf{B}_1}F^* - \mathbf{z}^{T\,\mathbf{B}_1}\mathbf{U}_{\mathbf{B}_2}{}^{\mathbf{B}_2}F - \tau_{f_{1r}}. \tag{39}$$

When the required acceleration is different from zero, mapping coefficients J_{2r} and J_{1r} can be solved from Eqs. (38) and (39).

VI. Stability Analysis for the System

This section presents the virtual stability analysis for the unactuated *open chain*. The virtual stability of the *object* and the entire system virtual stability are proven [9]. The stability analysis for a similar redundant hydraulic manipulator presented in [13].

A. Stability Analysis of the Unactuated Open Chain

The virtual stability of the unactuated *open chain* can be ensured by using Theorem 1 and Definition 2.16 in [12].

Theorem 1. *Consider the open chain, composed of two unactuated joints (joint 1 and joint 2) and two rigid links (link 1 and link 3), depicted in Fig. 2, described by Eqs.* (5)–(8) *and* (13)–(18)*, and with the control equations Eqs.* (20)–(23) *and* (29)–(34)*. This subsystem is virtually stable with its affiliated vector* $^{\mathbf{B}_j}V_r - {}^{\mathbf{B}_j}V, \forall j \in \{1,3\}$ *being a virtual function in* L_2 *and* L_∞ *in the sense of Definition 2.17 in [12].*

Proof. Let the non-negative accompanying functions v_{oc} for the studied *open chain* be

$$v_{\text{oc}} = v_{\mathbf{B}_1} + v_{\mathbf{B}_3}, \tag{40}$$

where $v_{\mathbf{B}_1}$ and $v_{\mathbf{B}_3}$ denote the non-negative accompanying functions for the rigid bodies of the unactuated *open chain* and are defined as

$$v_{\mathbf{B}_j} = \frac{1}{2}(^{\mathbf{B}_j}V_r - {}^{\mathbf{B}_j}V)^T\mathbf{M}_{\mathbf{B}_j}(^{\mathbf{B}_j}V_r - {}^{\mathbf{B}_j}V), \tag{41}$$

where $j \in \{1,3\}$ is the order number of the coordinate frame.

Subtracting Eq. (13) from Eq. (29) yields

$$\begin{aligned} ^{\mathbf{B}_j}F_r^* - {}^{\mathbf{B}_j}F^* &= \mathbf{M}_{\mathbf{B}_j}\tfrac{d}{dt}(^{\mathbf{B}_j}V_r - {}^{\mathbf{B}_j}V) \\ &+ \mathbf{C}_{\mathbf{B}_j}(^{\mathbf{B}_j}\omega)(^{\mathbf{B}_j}V_r - {}^{\mathbf{B}_j}V) + \mathbf{K}_{\mathbf{B}_j}(^{\mathbf{B}_j}V_r - {}^{\mathbf{B}_j}V). \end{aligned} \tag{42}$$

Further, the skew-symmetric property of $\mathbf{C}_{\mathbf{B}_j}(^{\mathbf{B}_j}\omega)$ yields

$$(^{\mathbf{B}_j}V_r - {}^{\mathbf{B}_j}V)^T\mathbf{C}(^{\mathbf{B}_j}\omega)(^{\mathbf{B}_j}V_r - {}^{\mathbf{B}_j}V) = 0. \tag{43}$$

Now, let the non-negative accompanying function for the unactuated *open chain* be written as

$$v_{\mathbf{B}_j} = \frac{1}{2}(^{\mathbf{B}_j}V_r - {}^{\mathbf{B}_j}V)^T\mathbf{M}_{\mathbf{B}_j}(^{\mathbf{B}_j}V_r - {}^{\mathbf{B}_j}V). \tag{44}$$

By differentiating Eq. (44), the time derivative of the $v_{\mathbf{B}_j}$ can be defined as

$$\begin{aligned}\dot{v}_{\mathbf{B}_j} &= ({}^{\mathbf{B}_j}V_r - {}^{\mathbf{B}_j}V)^T \mathbf{M}_{\mathbf{B}_j} \frac{d}{dt}({}^{\mathbf{B}_j}V_r - {}^{\mathbf{B}_j}V) \\ &= ({}^{\mathbf{B}_j}V_r - {}^{\mathbf{B}_j}V)^T \Big[({}^{\mathbf{B}_j}F_r^* - {}^{\mathbf{B}_j}F^*) - \\ &\quad \mathbf{C}({}^{\mathbf{B}_j}\omega)({}^{\mathbf{B}_j}V_r - {}^{\mathbf{B}_j}V) - \mathbf{K}_{\mathbf{B}_j}({}^{\mathbf{B}_j}V_r - {}^{\mathbf{B}_j}V) \Big] \\ &= -({}^{\mathbf{B}_j}V_r - {}^{\mathbf{B}_j}V)^T \mathbf{K}_{\mathbf{B}_j}({}^{\mathbf{B}_j}V_r - {}^{\mathbf{B}_j}V) \\ &\quad + ({}^{\mathbf{B}_j}V_r - {}^{\mathbf{B}_j}V)^T ({}^{\mathbf{B}_j}F_r^* - {}^{\mathbf{B}_j}F^*). \end{aligned} \tag{45}$$

Then, it follows from Definition 2.16 in [12] and Eqs. (5)–(8), (14)–(17), (18), (20)–(23), (30)–(33) and (34) that the last term in (45) can be expressed as

$$\begin{aligned}&({}^{\mathbf{B}_j}V_r - {}^{\mathbf{B}_j}V)^T ({}^{\mathbf{B}_j}F_r^* - {}^{\mathbf{B}_j}F^*) \\ &\quad = ({}^{\mathbf{B}_j}V_r - {}^{\mathbf{B}_j}V)^T \Big[({}^{\mathbf{B}_j}F_r - {}^{\mathbf{B}_j}F) - {}^{\mathbf{B}_j}\mathbf{U}_{\mathbf{B}_{j+1}} ({}^{\mathbf{B}_{j+1}}F_r - {}^{\mathbf{B}_{j+1}}F) \Big] \\ &\quad = \Big[{}^{\mathbf{B}_{j-1}}\mathbf{U}_{\mathbf{B}_j}^T ({}^{\mathbf{B}_{j-1}}V_r - {}^{\mathbf{B}_{j-1}}V) + \mathbf{z}(\dot{q}_{ir} - \dot{q}_1) \Big]^T ({}^{\mathbf{B}_j}F_r - {}^{\mathbf{B}_j}F) \\ &\qquad - \Big[{}^{\mathbf{B}_j}\mathbf{U}_{\mathbf{B}_{j+1}}^T ({}^{\mathbf{B}_j}V_r - {}^{\mathbf{B}_j}V) \Big]^T ({}^{\mathbf{B}_{j+1}}F_r - {}^{\mathbf{B}_{j+1}}F) \\ &\quad = ({}^{\mathbf{B}_{j-1}}V_r - {}^{\mathbf{B}_{j-1}}V)^T {}^{\mathbf{B}_{j-1}}\mathbf{U}_{\mathbf{B}_j} ({}^{\mathbf{B}_j}F_r - {}^{\mathbf{B}_j}F) \\ &\qquad + (\dot{q}_{ir} - \dot{q}_i)\mathbf{z}^T ({}^{\mathbf{B}_j}F_r - {}^{\mathbf{B}_j}F) \\ &\qquad - ({}^{\mathbf{B}_{j+1}}V_r - {}^{\mathbf{B}_{j+1}}V)^T ({}^{\mathbf{B}_{j+1}}F_r - {}^{\mathbf{B}_{j+1}}F) \\ &\quad = p_{\mathbf{B}_{j-1}} - p_{\mathbf{B}_{j+1}} + (\dot{q}_{ir} - \dot{q}_i)\mathbf{z}^T ({}^{\mathbf{B}_j}F_r - {}^{\mathbf{B}_j}F), \end{aligned} \tag{46}$$

where $p_{\mathbf{B}_{j+1}}$ and $p_{\mathbf{B}_{j-1}}$ are virtual power flows (VPFs) (see Definition 2.16 in [12]). In view of Eqs. (19), (18), and (34), the last term in (46) can be written as

$$\begin{aligned}&(\dot{q}_{ir} - \dot{q}_i)\mathbf{z}^T ({}^{\mathbf{B}_j}F_r - {}^{\mathbf{B}_j}F) \\ &\quad = -(\dot{q}_{ir} - \dot{q}_i)\Big[k_{vi}(\dot{q}_{ir} - \dot{q}_i) + k_{ci}(\tanh(n\dot{q}_{ir}) - \tanh(n\dot{q}_i)) \Big] \\ &\quad = -k_{vi}(\dot{q}_{ir} - \dot{q}_i)^2 - (\dot{q}_{ir} - \dot{q}_i)k_{ci}(\tanh(n\dot{q}_{ir}) - \tanh(n\dot{q}_i)), \end{aligned} \tag{47}$$

where

$$(\dot{q}_{ir} - \dot{q}_i)k_{ci}(\tanh(n\dot{q}_{ir}) - \tanh(n\dot{q}_i)), \geq 0 \tag{48}$$

holds $\forall i \in \{1,2\}$.

Then, taking the time derivative from (40) and by using Eqs. (45)–(48), $\forall i \in \{1,2\}$, and $\forall j \in \{1,3\}$, yields

$$\begin{aligned}\dot{v}_{\text{oc6}} &= \dot{v}_{\mathbf{B}_1} + \dot{v}_{\mathbf{B}_3} \\ &\leq -({}^{\mathbf{B}_1}V_r - {}^{\mathbf{B}_1}V)^T \mathbf{K}_{\mathbf{B}_1} ({}^{\mathbf{B}_1}V_r - {}^{\mathbf{B}_1}V) \\ &\quad -({}^{\mathbf{B}_3}V_r - {}^{\mathbf{B}_3}V)^T \mathbf{K}_{\mathbf{B}_3} ({}^{\mathbf{B}_3}V_r - {}^{\mathbf{B}_1}V) \\ &\quad -k_{v1}(\dot{q}_{1r} - \dot{q}_1)^2 - k_{v3}(\dot{q}_{3r} - \dot{q}_3)^2 \\ &\quad + p_{\mathbf{B}_0} - p_{\mathbf{B}_4}, \end{aligned} \tag{49}$$

Consider that the *open chain* has one *driven* VCP associated with frame $\{\mathbf{B}_0\}$ and one *driving* VCPs associated with frame $\{\mathbf{B}_4\}$. Using (40), (41), and (49) completes the proof of the *virtual stability* of the unactuated *open chain*, in the sense of Definition 2.17 in [12], ensuring that ${}^{\mathbf{B}_j}V_r - {}^{\mathbf{B}_j}V \in L_2 \bigcap L_\infty, \forall j \in \{1,3\}$, and $(\dot{q}_{ir} - \dot{q}_i) \bigcap L_\infty, \forall i \in \{1,2\}$. □

TABLE I
VDC CONTROLLER FEEDBACK GAINS

Lift cylinder	Tilt cylinder	Extension cylinder
λ_x = 35.6 $[\frac{m}{s}]$	λ_x = 35 $[\frac{m}{s}]$	λ_x = 36 $[\frac{m}{s}]$
k_f = 4.3·10^{-6} $[\frac{m^2}{Ns}]$	k_f = 5·10^{-6} $[\frac{m^2}{Ns}]$	k_f = 2.6·10^{-6} $[\frac{m^2}{Ns}]$
k_x = 0.041 [m]	k_x = 0.039 [m]	k_x = 0.025 [m]

B. Stability Analysis of the Entire System

The entire system is stable in view of Theorem 2.1 in [12], if all the subsystems are proof of the virtual stability, and all the VPF's can be canceled out in the summation of the time derivative of all non-negative accompanying functions, in view of Lemma 2.3 in [12]. The virtual stability of the *object* is proven in [9], and the virtual stabilities of the remaining subsystems (manipulator subsystems; see Fig. 2a) are proven in [13].

VII. Experimental Results

The experiments, with a full-scale commercial Hiab 033 hydraulic manipulator (see Fig. 1), demonstrated the control performance of the proposed anti-sway controller. The experimental setup consisted of the following hardware components:

1) PowerPC-based dSpace ds1103 with sample time of 1 ms
2) Bosch Rexroth NG6 size servo solenoid valve (40 l/min at Δp = 3.5 MPa per notch) for Lift cylinder
3) Bosch Rexroth NG10 size servo solenoid valve (50 l/min at Δp = 3.5 MPa per notch) for Tilt cylinder
4) Bosch Rexroth NG10 size servo solenoid valve (100 l/min at Δp = 3.5 MPa per notch) for Extension cylinder
5) Lift and Tilt cylinder dimensions: ϕ80/60–607
6) Extension cylinder dimensions: ϕ45/30–1350
7) Druck PTX1400 pressure transmitter (range 25 MPa)
8) Fraba Incremental encoders (16384 inc/rev)
9) Vahva B15 (mass 90 kg) gripper and a load mass 150 kg
10) Unactuated rigid links l_1 = 0.13 m and l_2 = 0.21 m

Control laws for the hydraulic cylinders of the manipulator are given in [13]. Table I shows the feedback gains for the lift, tilt, and extension cylinders used in the present study. In Table I, λ_x, k_x and k_f are the cylinder's piston position, velocity, and force feedback gains. The joint position feedback gains in Eq. (24) were λ_{u_1} = 28 and λ_{u_2} = 18.

In the experiments, the proposed anti-sway controller was demonstrated in a case study of redundant vertical plane motion. A freely swaying motion of the manipulator tip is generated by designing a point-to-point quintic reference trajectory, which is generated for motions along the *x*-axis (see Fig. 1). Fig. 4 presents the results for the compensated and uncompensated systems, when the load center of mass moves from position 2.3 m to 2.7 m in 1.2 s. The solid line denotes the desired position trajectory, the dashed line denotes the results to anti-sway compensation, and the dotted line denotes the results without damping control (the manipulator was controlled with a well-tuned p-control). Fig. 4 shows that the proposed anti-sway controller can efficiently damp the swaying of the load. The settling time (2% from the final

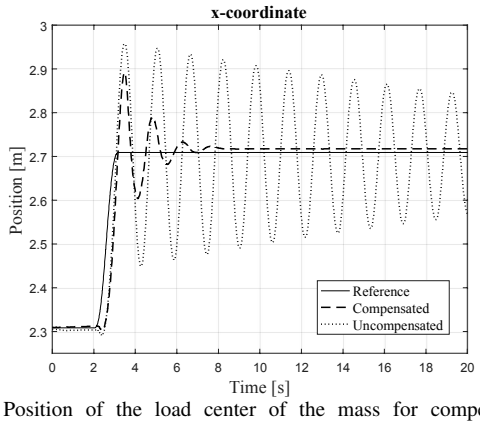

Fig. 4. Position of the load center of the mass for compensated and uncompensated system with a 1.2 s ramp

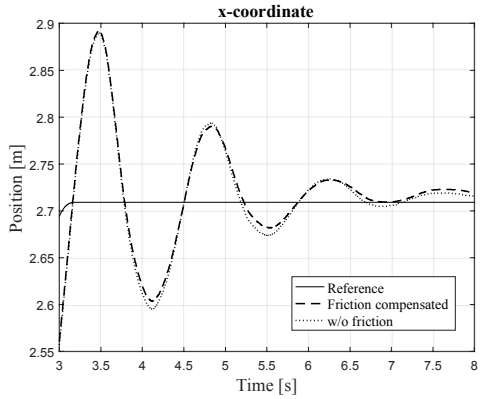

Fig. 5. Load position with and without the friction model

value) for the anti-sway controlled system is approximately 3 s, when the corresponding settling time for the uncompensated system is more than 20 seconds. The persistent overshoot of the compensated system is approximately 7%, which is less than the overshoot of the uncontrolled system. By comparing our previous results in [9] to Fig. 4, it can be observed that faster ramp does not affect to the settling time.

Fig. 5 shows the effect of the proposed friction model to the load damping with the same trajectory as in Fig. 4. The dashed line presents the results with the friction model, and the dotted line shows the results without the friction model in view of our previous study [9]. As Fig. 5 shows the friction model effect to compensate for the swaying of the load. As Fig. 4 shows, without an anti-sway controller the first unactuated joint is lightly very damped. For that reason, the friction model effects on the damping of the load are low in this case. The friction model is more significant in cases where the load mass affects the damping less.

VIII. Conclusions

This paper proposed, for the first time, a nonlinear full model-based anti-sway control method for the coordinate controlled redundant hydraulic manipulator. Furthermore, the stability of the proposed anti-sway controller was guaranteed in stability analysis. The experiments, with a full-scale coordinate controlled redundant hydraulic manipulator, verify that the proposed anti-sway controller damps the swaying of the load efficiently. In this case, the proposed friction model effect on the load damping is low, because of the lightly damped joints.

In future studies, the proposed anti-sway control method will be implemented to damp the load swaying motions in both unactuated directions. As demonstrated in [14], [15], the parameter adaption for uncertain parameters (e.g., in friction and rigid body dynamics) can significantly improve the control performance of hydraulic systems. In future studies, the parameter adaption will be incorporated. Furthermore, the proposed anti-sway controller will be extended to cover asymmetric loads.

Acknowledgment

This work was supported by the Academy of Finland under the project "CPS-based supervision and control of flexible link manipulators" grant no. 294915.

References

[1] J. Mattila, J. Koivumäki, D. G. Caldwell, and C. Semini, "A survey on control of hydraulic robotic manipulators with projection to future trends," *IEEE/ASME Transactions on Mechatronics*, vol. 22, no. 2, pp. 669–680, 2017.

[2] John Deere, *Inteligent Boom Control*, 2013, [online], accessed 26.6.2017, available: www.deere.com/en_US/corporate/our_company/news_and_media/press_releases/2013/forestry/2013oct17_intelligent_boom_control.page.

[3] HIAB, *Crane Tip Control*, 2017, [online], accessed 26.6.2017, available: www.hiab.com/en/company/newsroom/news/hiab-crane-tip-control/.

[4] F. Palis and S. Palis, "Modelling and anti-sway control of rotary cranes," in *Power Electronics and Motion Control Conference (EPE/PEMC), 2010 14th International*. IEEE, 2010, pp. T5–163.

[5] H. Ouyang, G. Zhang, L. Mei, X. Deng, and D. Wang, "Load vibration reduction in rotary cranes using robust two-degree-of-freedom control approach," *Advances in Mechanical Engineering*, vol. 8, no. 3, p. 1687814016641819, 2016.

[6] N. Uchiyama, "Robust control of rotary crane by partial-state feedback with integrator," *Mechatronics*, vol. 19, no. 8, pp. 1294–1302, 2009.

[7] M. B. Kjelland, M. R. Hansen, I. Tyapin, and G. Hovland, "Tool-point control of a planar hydraulically actuated manipulator with compensation of non-actuated degree of freedom," in *Proc. IEEE 12th Int. Conf. on Control, Automation and Systems (ICCAS)*, 2012, pp. 672–677.

[8] J. Neupert, E. Arnold, K. Schneider, and O. Sawodny, "Tracking and anti-sway control for boom cranes," *Control Engineering Practice*, vol. 18, no. 1, pp. 31–44, 2010.

[9] P. Mustalahti, J. Koivumaki, and J. Mattila, "Stability-guaranteed anti-sway controller design for a redundant articulated hydraulic manipulator in the vertical plane," in *ASME/BATH 2017 Symposium on Fluid Power and Motion Control*, 2017, [Accepted].

[10] J. Kalmari, J. Backman, and A. Visala, "Nonlinear model predictive control of hydraulic forestry crane with automatic sway damping," *Computers and Electronics in Agriculture*, vol. 109, pp. 36–45, 2014.

[11] W.-H. Zhu, Y.-G. Xi, Z.-J. Zhang, Z. Bien, and J. De Schutter, "Virtual decomposition based control for generalized high dimensional robotic systems with complicated structure," *IEEE Trans. Robot. Autom.*, vol. 13, no. 3, pp. 411–436, 1997.

[12] W.-H. Zhu, *Virtual decomposition control: toward hyper degrees of freedom robots*. Springer Science & Business Media, 2010, vol. 60.

[13] J. Koivumäki and J. Mattila, "High performance nonlinear motion/force controller design for redundant hydraulic construction crane automation," *Automation in Construction*, vol. 51, pp. 59–77, 2015.

[14] W.-H. Zhu and J.-C. Piedboeuf, "Adaptive output force tracking control of hydraulic cylinders with applications to robot manipulators," *ASME J. Dyn. Syst., Meas., Control*, vol. 127, no. 2, pp. 206–217, 2005.

[15] J. Koivumäki and J. Mattila, "Adaptive and nonlinear control of discharge pressure for variable displacement axial piston pumps," *ASME J. Dyn. Syst., Meas., Control*, vol. 139, no. 10, 2017.